Scientific Research Publishing

Open Journal of Applied Sciences, 2025, 15(9), 2707-2723
https://www.scirp.org/journal/ojapps
ISSN Online: 2165-3925
ISSN Print: 2165-3917

Lighting the Wounds: How LED Technology Could Revolutionize Early Detection of Buruli Ulcer

Didier Konan Yable[1,2*], Abdoulaye Kadiolotien Soro[1], Kouakou Rodolphe Kossonou[1], Olivier Asseu[1,2], Cissé Theodore Haba[2]

[1]LASTIC, ESATIC, Abidjan, Côte d'Ivoire
[2]INP-HB, Yamoussoukro, Côte d'Ivoire
Email: *didier.yable@esatic.edu.ci

How to cite this paper: Yable, D.K., Soro, A.K., Kossonou, K.R., Asseu, O. and Haba, C.T. (2025) Lighting the Wounds: How LED Technology Could Revolutionize Early Detection of Buruli Ulcer. *Open Journal of Applied Sciences*, **15**, 2707-2723.
https://doi.org/10.4236/ojapps.2025.159182

Received: August 4, 2025
Accepted: September 15, 2025
Published: September 18, 2025

Abstract

Our research focuses on the detection of *M. ulcerans* (*Mycobacterium ulcerans*), etiological agent of Buruli ulcer, and the analysis of the spectra of the optical properties of human skin by diffuse reflectance spectroscopy. This promising technique is established in this paper for non-invasive and *in vivo* characterization of optical properties of tissues for diagnostic application. An innovative, compact and low-cost architecture for DRS (Diffuse Reflectance Spectroscopy) has been proposed. This innovative approach is based on the use of a multispectral image sensor and LEDs (Light-Emitting Diode) to obtain a diffuse reflectance signal in contact with the skin. This prototype, including a spectrometer coupled to an optical fiber, a microcontroller, an array of 8 LEDs and a computer, has been developed, fabricated and implemented. Diffuse reflectance profiles were acquired at 438 nm, 544 nm and 613 nm. The spectrum of *M. ulcerans* was established by this method at 256 nm and 365 nm. The results obtained confirm the potential and of our approach for quantitative tissue information and study of Buruli ulcer disease progression before changes are visibly apparent. This suggests the possibility of using it as a complementary technique to clinical assessment.

Keywords

Diagnostics, Diffuse Reflectance, *Mycobacterium ulcerans*, Skin

1. Introduction

Buruli Ulcer (BU) of etiological agent *Mycobacterium ulcerans*, is a necrotic, infection and debilitating bacterial disease. The incidence of BU is proliferating

worldwide and ranks as the third most neglected tropical disease according to the World Health Organization [1]-[3]. Clinically, this infection often starts with a nodule, papule or edema without systematic symptoms. Then, the disease progresses to necrotic ulcers and open wounds, finally evolving to scarring, contractures and deformities with possible total loss of joint function [4]-[6]. The absence of pain at the site of the lesions in the early stages of infection leads to a delay in seeking care in most cases. However, BU can be treated if diagnosed at an early stage. If not, the consequences are dramatic, because this Mycobacterium destroys the flesh and, at an advanced stage, the only possible medical outcome is major surgery or amputation of the affected limb.

Ivory Coast and Indonesia are two countries heavily affected by this disease. Most diagnostic tests in the field today use invasive methods, which require state-of-the-art equipment and relatively expensive test kits.

This method can result in physical pain and even risk of infection. The development of a cost-effective, biopsy-free device for early diagnosis of Buruli ulcer is of paramount importance in the fight against this disease but also to improve our understanding. We are looking for an innovative and cost-effective technique based on the optical detection of the signatures of this Mycobacterium. In this way, the knowledge of the optical properties of the skin constitutes a major stake in the management of patients for many pathologies. Instruments capable of measuring these properties *in vivo* and in a non-invasive way are very much in demand, both by the medical profession and by the cosmetic industry.

In this scientific context, optical imaging methods have gained popularity in recent years due to their more objective ability to assist the patient in many processes by probing tissue properties in an objective and reliable manner [7]. These techniques are based on light-matter interaction in the visible and near-infrared spectral regions with skin constituents to determine biochemical and morphological properties. These properties can in turn be related to functional parameters useful to the practitioner. Thus, diffuse reflectance spectroscopy (DRS), a spectroscopic method with considerable potential in medical diagnosis, [8] has been widely used to determine the absorption and scattering properties of cloudy or turbid media. When applied to biological tissues such as skin, DRS allows quantitative characterization of cellular and subcellular tissue composition and tissue chromophore types and concentrations for noninvasive medical diagnosis. In the visible and near-infrared range, these chromophores include oxyhemoglobin, deoxyhemoglobin, melanin, and bilirubin, which are of great interest in various clinical situations.

Many groups have already investigated DRS as a non-invasive tool to provide *in vivo* diagnostic criteria. Many studies have reported that DRS is a rapid, non-invasive and very important technique in many biomedical applications such as monitoring tissue oxygenation [9] [10] evaluation of tumor margin in epithelium [11] detection of breast or colon cancer [12] diagnosis of jaundice in newborns skin pharmacokinetics [13] [14] etc. DRS provides information about the absorption and diffusion properties of the tissue in depth and in a quantitative way. Moreover,

this technique can be realized through compact and relatively inexpensive devices, which is a clear advantage in many biomedical applications. However, the translation of this technology is still hampered by some difficulties. In particular, the integration of the instruments into routine hospital procedures and their ability to adapt to the variety of tissues encountered *in vivo*. In particular, the characterization of the properties of the distinct layers of the skin, epidermis and dermis, can be useful for diagnostic applications. We propose implementing this approach using portable and low-cost technologies, integrating a system associated with LEDs (Light-Emitting Diode) illumination to limit the impact of the instrument in terms of cost and size. Recently, the bacteriological diagnosis of *Mycobacterium tuberculosis* based on LED microscopy has improved the sensitivity and speed of techniques. Thus, the new LED fluorescence microscopes replace light microscopes and Ziehl-Neelsen staining. This makes Ziehl-Neelsen staining examination more sensitive, faster and easier. LEDs are excellent candidates for general lighting because of their efficiency, reliability, and expected bulb life (up to 50,000 h); they produce little heat and do not contain hazardous materials [15]. This is a significant advantage and improvement. We will first show the experimental setup in this proposed model. Then we will present our preliminary results Finally, we validate *in vivo* the relevance of this approach, by further measurements performed on three selected skin sites with LED sources. The satisfactory results obtained are presented in this article showing the feasibility in clinics.

2. Materials and Methods

2.1. Experimental Installation

For a characterization of M. ulcerans, we have designed a spectroscopy system. A prototype consisting of a standard resolution optical sensor to obtain the spectral signature of this bacterium in contact mode (**Figure 1**) has been developed. To evaluate the potential of our approach, a prototype instrument was designed and fabricated in the LAPLACE laboratory. The instrument consists of a commercially available optoelectronic sensor combined with a fiber optic coupling system. The coupling system uses 8 surface-mounted light emitting diodes (LEDs) and a fiber optic (FOP), ensuring efficient transfer of photons over the array. The short pass filter UG11 and long pass filter GG420 are used to isolate a certain spectral range. The reflectance signals of interest are collected using a circular G11 short pass filter made of colored glass (purple color) suppressing the wavelengths below 400 nm and 700 nm. And long pass filter GG420 circular colored glass (blue color) collects reflectance signals of interest above 400 nm. This system has been developed to produce and collect diffuse reflectance models in contact imaging mode. We described the design of the instrument, presented the developed prototype and finally evaluated the performance of the prototype on tissue mimicking optical phantoms. A total of nine volunteers were recruited, including individuals with healthy skin and skin areas located near Buruli ulcer lesions, forming two categories, person A and person B. All participants were informed of the objectives and

procedures of the study.

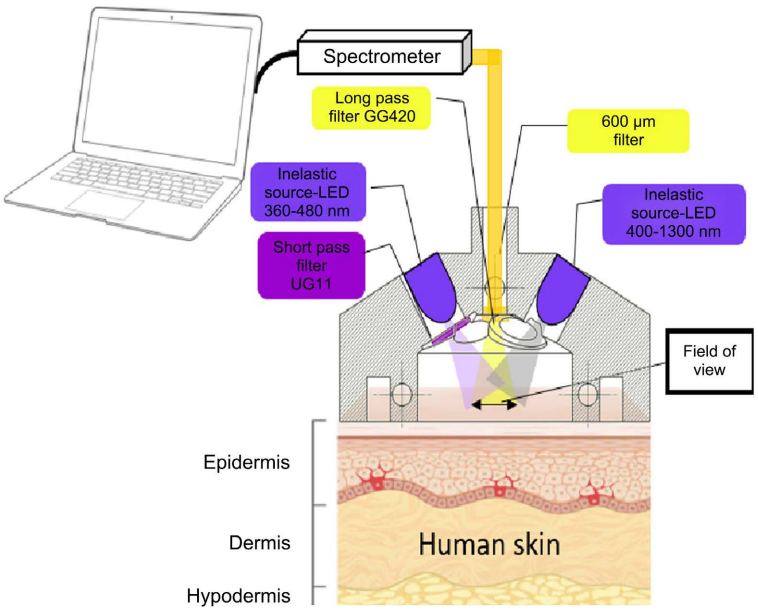

Figure 1. Schematic diagram of the experimental configuration used for the acquisition of the spectra.

2.2. Brightness Sensor

To sample the reflectance of turbid or turbid media, we used to an eight-bite spectrometer to detect and record the spectra of backscattered light on the surface of the tissue, an optical fiber, a set of LEDs, a deuterium lamp as an excitation source (**Figure 1**). In addition, a PC was used for precise control of the acquisition of the measurements in less than five seconds and for processing the acquired data to extract the absorption and scattering properties of the tissue. Validation experiments were conducted on human subjects following the methodology used by other authors [12] [13] and using diffuse reflectance sampled from the scattering media.

No studies have been performed to obtain results on individuals based on age, gender, or ethnicity, which could be related to skin color and tissue scattering or analysis.

No subject has been excluded for the use of sunscreen, body lotion or medication, or for the presence of tattoos or skin conditions or disorders. The measurements session consisted of collecting a spectrum of the test area on the subject's limbs and acquiring reflectance measurements of the test area. This test area was chosen for practical reasons, namely the ease of measurements with the spectrophotometer. The most intuitive approach is to place the sensor itself in contact with the tissue to collect and detect scattered photons, as proposed in [16] [17].

3. Measurements and Characterizations

Diffuse reflectance is a fast non-invasive technique that allows to characterize the optical parameters of the analyzed skin and quantify the phenomena of diffusion

and absorption of light. Thus, the processes of reflectance measurements of the subject's limb skin were acquired using an ultraviolet/visible/neo-infrared spectrophotometer (Ocean Optics spectrometer) operating in the spectral region of 360 to 1300 nm. We first adjusted the integration time so that the peak was at about 85% of the maximum. The illumination source is a set of eight LEDs (Light-Emitting Diode) as excitation source with wavelengths 360 nm, 365 nm, 530 nm and 610 nm. In addition, we used these LEDs to generate the desired diffuse reflectance signals. Each type of LED is positioned symmetrically on the periphery of a semi-circle. They are bent at a 45˚ angle to evenly illuminate the test area. LEDs are available on many wavelengths, are very miniaturized and inexpensive, which reduces the size and cost DRS system. We chose the different ones considering the reflectivity of the epidermis, which is 20% (**Figure 2**) at 470 nm and 530 nm. We also considered the main absorbers of the dermis, which are hemoglobin with maxima at 420 nm, 540 nm for oxyhemoglobin [16] [17]. The hypodermis, the deep layer of the skin, has not been mentioned here, because our device does not reach this depth. The protocol was approved based on studies conducted by the relevant ethics committee [18]. Three diffuse reflectance measurements were taken without prior application of any product for each skin site on the nine volunteers, using our dedicated instrument. Finally, the spectra obtained were then processed and analyzed in an Excel spreadsheet to extract the parameters of interest.

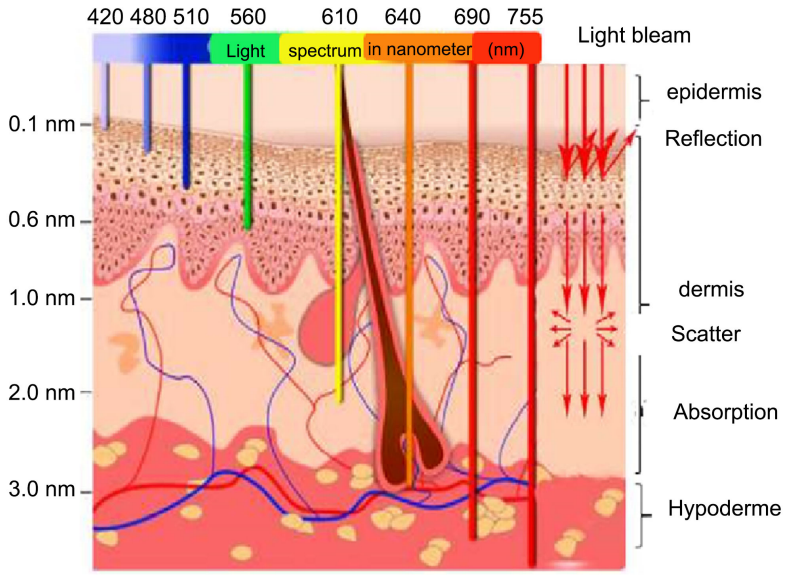

Figure 2. Depth of light penetration into skin tissue for different wavelengths.

Wavelengths such as 360 nm were chosen considering the absorption region of *M. ulcerans* in the ultraviolet and hemoglobin with maxima at 420 nm and 540 nm. Beyond 650 nm, the results obtained show negative reflectance peaks, which have no desirable or exploitable physical significance.

Each selected LED wavelength (360 nm, 420 nm, and 540 nm) was chosen to specifically target the ultraviolet absorption of bacterial aromatic compounds, the

maximum absorption of the dermis, and that of oxyhemoglobin.

4. Reflectance Factor Analysis and Uncertainty Assessment

The spectral reflectance factor of a given skin tissue sample at each wavelength can be calculated from the following equation:

$$R(\lambda)=\frac{s(\lambda)-s_d(\lambda)}{s_s(\lambda)-s_d(\lambda)}\times R \tag{1}$$

where S is the signal intensity of a skin sample wavelength scan λ, S_s is the reference signal of a standard λ, S_d is the spectrum of the length λ and R_s is the spectral reflectance factor of standard λ. In addition, the *Spectra-Suite* software internally substitutes and calculates the relative intensity percentage 85% of a standard reference blank by this equation:

$$(\%)R=\frac{s(\lambda)-s_d(\lambda)}{s_s(\lambda)-s_d(\lambda)} \tag{2}$$

where S is the intensity of the signal from a scan of the skin sample at the wavelength λ, S_d is the dark intensity of at the wavelength λ, S_s is the reference intensity at wavelength λ. To obtain these results, the analysis procedure is such that two spectra must first be recorded: the reference spectrum S_s and the dark (noise) spectrum. S_d The reference spectrum contains the emission curve of the source, the response of the array, the photodetector, the absorption of any filters and the ambient signal. The dark spectrum contains the stray light and the dark (noise) signal of the photodetector. Table 1 and Table 2 summarize the data obtained. Following the data obtained, we studied the optical properties of the skin.

Table 1. Wavelength as a function of absorbance.

Wavelength [nm]	Absorbance
210	0.25
256	0.3
365	0.35

Table 2. Optical parameters of human skin of epidermis, thickness $l_{rpi}=100$ μm .

WI [nm]	Refra Idx	Anis g	$\mu_{a,mel}$ 100 mm^{-1}	$\mu_{a,skin}$ 100 mm^{-1}	μ_a 100 mm^{-1}	μ_s 100 mm^{-1}
360	1.356	0.724	20.28	4..04	406	148.35
365	1.354	0.725	19.37	3.76	388	141.36
420	1.343	0.742	12.14	1.79	243	87.93
430	1.342	0.745	11.22	1.56	225	80.93
470	1.338	0.756	8.35	0.96	167	60.61
530	1.335	0.774	5.594	0.535	112	41.99
580	1.333	0.788	4.143	0.381	83.2	31.99
1310	1.323	0.999	0.275	0.275	5.70	4.900

5. Optical Properties of the Skin

5.1. Calculation of the Absorption Coefficients of the Skin Layers

To quantify possible changes in physiological parameters due to the presence of disease, a study of images of healthy skin was necessary.

Thus, the optical skin model was first validated on normal subjects. **Figure 1** shows the measurements made on the left form of a healthy subject.

Then, the biological medium was described using optical properties such as the absorption coefficient μ_a, the scattering coefficient μ_s, the refractive index of the medium n and the anisotropy factor g. At the macroscopic scale, human tissues being considered as layers, we used a simplified mathematical model for each layer considered in our analysis.

For the epidermis, melanin is the main contribution, and for the dermis, the model mainly considers blood volume and blood oxygenation.

5.2. Epidermal Layer

The effect of thin epidermal layer on the intensity of diffusely reflected light is based on the volume of melanin in the epidermis and the thickness of the epidermis [2]. The effective attenuation of light through the epidermis, A_{epi} is determined by the Beer-Lambert law, which gives:

$$A_{epi}(\lambda) = \exp\left[-\mu_{a,epi}(\lambda) l_{epi}\right]. \tag{3}$$

where λ is the wavelength in nm, $\mu_{a,epi}$ the absorption coefficient of the epidermis in mm^{-1}, and l_{epi} the thickness of the epidermis in mm. The total absorption coefficient of the epidermis, μ_{epi} depends on the percentage or volume fraction of melanin in the skin and is given by:

$$\mu_{a,epi}(\lambda) = f_{mel} \cdot \mu_{a,mel}(\lambda) + (1 - f_{mel}) \mu_{a,skin}(\lambda). \tag{4}$$

With f_{mel} the volume fraction of melanin according to skin tone, $\mu_{a,mel}$ the melanin absorption coefficient, and $\mu_{a,skin}$ the absorption coefficient of normal skin excluding base melanin. The results presented in this paper are based on the previously reported values for $\mu_{a,mel}$ [3] and $\mu_{a,skin}$ [4], see **Table 2**.

The remaining variable is the volume fraction fmel melanin in the epidermis. The absorption coefficient for normal skin was considered to be the same for the epidermal and dermal layers. This model does not take into account epidermal scattering because the probability of a scattering event in a 60 μm epidermis is very low, less than 5%. The absorption coefficients for melanin and dermal layer can be approximated as follows:

$$\mu_{a,mel}(\lambda) = 6.6 \times 10^{11} \lambda^{-3.33} \tag{5}$$

and

$$\mu_{a,skin}(\lambda) = 0.244 + 85.3 \exp\left[\frac{-(\lambda - 154)}{66.2}\right] \tag{6}$$

Gemert [5] proposed an empirical skin equation that relates the anisotropy fac-

tor g to wavelength. Epidermal anisotropy factors g_{epi} the dermis g_{der} given by:

$$g_{skin} = g_{epi} = g_{der} = 0.62 + 0.29 \times 10^{-3} \lambda \tag{7}$$

where λ is the wavelength. The refractive indices [6] are calculated by:

$$n(\lambda) = 1.3199 + 6878\lambda^{-2} - 1.32 \times 10^{9} \lambda^{-4} + 1.11 \times 10^{14} \lambda^{-6} \tag{8}$$

5.3. Dermal Layer

For the dermis, the thickest and most diffusive layer, its influence on the skin reflectance is estimated by a stochastic model of photon migration, e.g., random walk theory. Given the known random walk expression for diffuse reflectivity, R_0 semi-infinite medium with an absorbent limit and without index shift [7]:

$$R_0(\lambda) = \frac{\exp(-2\mu)}{\sqrt{42\mu}}\left[1 - \exp\left(-\sqrt{24\mu}\right)\right] \tag{9}$$

where μ is the ratio of the absorption and diffusion coefficients $\frac{\mu}{\mu'}$. In the case of the dermis:

$$\mu = \frac{\mu_{dermis}}{\mu'} \tag{10}$$

μ_{dermis} and μ' are the reduced diffusion and absorption coefficients of the dermis, respectively. The attenuation coefficient of this layer is related to the volume fraction of blood in the tissue and the percentage of oxygenated blood given:

$$A_{dermis}(\lambda) = 1.06 - 1.45\left[\frac{\mu_{dermis}}{\mu'}\right]^{0.35} \tag{11}$$

The dermal absorption coefficient depends on the contribution of the volume fraction of blood in the tissue, blood and the percentage of that blood that is oxygenated foxy relative fractions of HbO_2 and Hb in the blood. The dermal absorption coefficient is calculated by:

$$\mu_{a,dermis}(\lambda) = f_{blood}\mu_{a,blood}(\lambda) + (1 - f_{blood})\mu_{a,skin}(\lambda) \tag{12}$$

Where blood is the volume fraction of blood in the dermal layer and $\mu_{a,skin}$ is the absorption coefficient of the skin. The absorption coefficient of whole blood is expressed as:

$$\mu_{a,blood}(\lambda) = f_{blood}\mu_{a,oxy}(\lambda) + (1 - f_{blood})\mu_{deoxy}(\lambda) \tag{13}$$

Data measured *in vitro* tend to be higher than those measured *in vivo* [8]. This may result from differences in sampling conditions and measurements methods used [9].

Table 2 clearly shows that the diffusion and absorption coefficients depend on the wavelength. Based on this observation, Jacques *et al.* have developed an empirical equation that represents the reduced diffusion coefficient μ_s of the dermis as a function of wavelength [10]. This equation is as follows:

$$\mu_s(\lambda) = 2 \times 10^{5} \lambda^{-1.5} + 2 \times 10^{12} \lambda^{-4} \tag{14}$$

Where the first term is Mie scattering and the second is Rayleigh scattering, λ

expressed in nanometer. The optical parameters calculated at different wavelengths are presented in Table 2. In the analysis, rather than assuming the constant anisotropy coefficient, whatever the sample analyzed, it is necessary to evaluate it according to the wavelength, this characterizes a better accuracy of the sampling step.

6. Results and Discussions

In this section, we first present our simulation results and then the results of the measurements carried out. Our simulation results show that the tissue light interaction is strongly wavelength-dependent and depending on the wavelength value, the light wave will propagate deeply inside the tissue, see Figure 3. Figure 4 and Figure 5 show the absorption spectrum of the epidermis and that of oxyhemoglobin in relation to wavelength, respectively.

This fluctuation in the index of cellular components such as cytoplasm and nuclei can be approximated to 1.3 in our study. This is obviously an order of magnitude; we do not attempt to be more precise because this value may vary in situ given the variability of the optical properties of the skin from one individual to another.

Figure 5 shows the elevation of fully oxygenated and fully deoxygenated blood. The absorbance spectra of oxyhemoglobin and deoxyhemoglobin, the major chromophores of the skin dermis in the ultraviolet, visible and infrared regions.

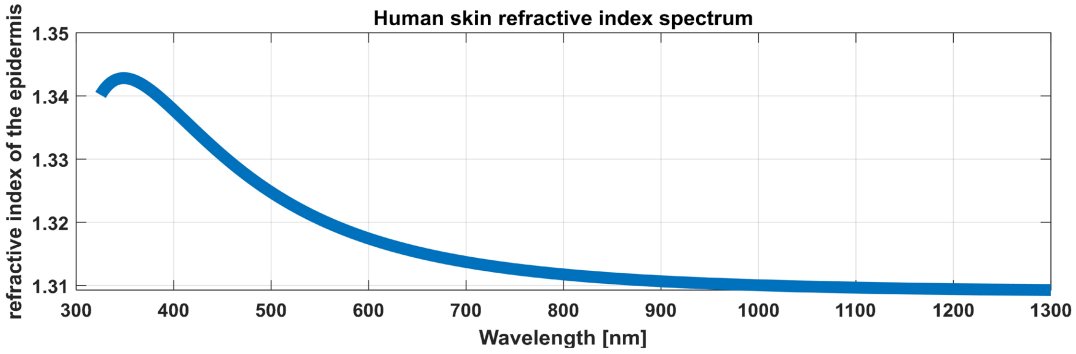

Figure 3. Refractive index of human skin as a function of wavelength.

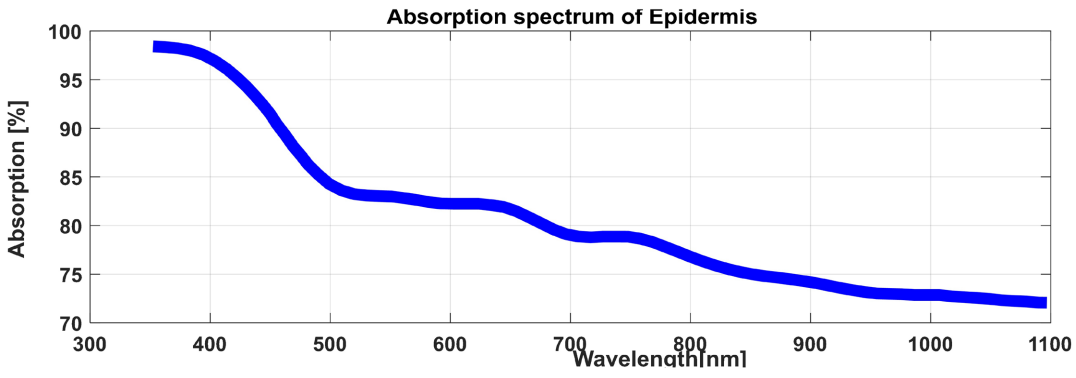

Figure 4. Absorption spectrum of the epidermis as a function of wavelength.

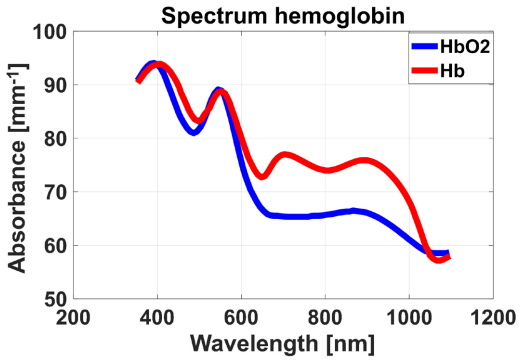

Figure 5. Absorption spectrum of oxyhemoglobin and deoxyhemoglobin as a function of wavelength at 430 nm and 580 nm.

Knowledge of the refractive index is therefore necessary to calculate the scattering properties, as the tissues are heterogeneous in composition. On the epidermal layer of the skin, at the wavelength of 350 nm, see Figure 6.

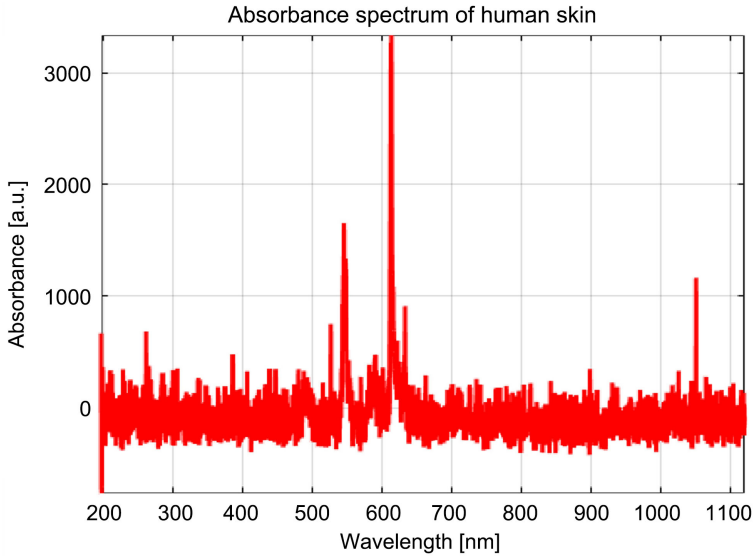

Figure 6. Reflectance spectrum of healthy human skin at 544 nm and 613 nm.

These preferred wavelengths must be absorbed by the target. The absorption coefficient, the probability per unit path length that a photon at a particular wavelength will be absorbed is a function of the concentration of chromophores present.

We obtained a strong absorption in the 420 nm (blue), 430 nm (green) and 580 nm (yellow) wavelengths and a weak but significant absorption band in the 800 nm to 1000 nm spectral region. This analysis allowed us to distinguish the less penetrating wavelengths of far UV and far infrared radiation due to proteins and water chromophores respectively.

There are many photothermal effects, as light cannot impose a tissue effect when it is absorbed by the chromophores of the medium. This study allowed us to find the discriminating frequencies and favored the choice of different lengths

for the study system.

The measurements were obtained from a continuous signal. The results of our experiment were simulated using **Matlab** and Excel 2016 software, as shown in Figure 6. Our experiment showed that the signal intensity passes through various tissue structures. We noticed that the structures are made up of peaks that represent echoes of different layers of light.

Three significant peaks are in the spectral region of 400 to 750 nm the presence of spurious noise. These spurious signals are caused by losses in the absorption and scattering of light relative to the wavelength used. The observed peaks are at 438 nm, 544 nm and 613 nm respectively.

This shows that normal skin with a non-ulcerative pimple absorbs more light in the visible region. These peaks are signals of the type of cellular chromophores present in the cytoplasm of the epidermis. During diagnosis, the practitioner could consider these wavelengths which would allow to better orient the characterization of this bacterium. We therefore clarified and reframed the measurement range. To prove the relevance of our approach, we prepared a phantom medium, *i.e.*, an inert physical device reproducing some properties of *M. ulcerans*. Figure 7 shows the absorption spectra specific to mycolactone A/B. It demonstrates the distinctive optical features of this molecule.

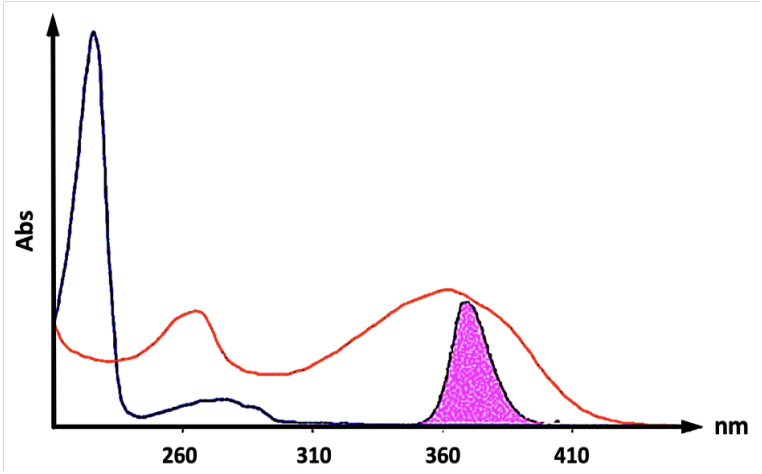

Figure 7. MeOH absorption spectra. Red: mycolactone A/B, Blue: 2-naphthylboronate with syn-2,4 pentanediol, transparent region through the 365 nm filter [11].

These methods for detection of Mycobacterium were used by thin layer chromatography (TLC) with irradiation through a 365 nm UV filter. Figure 8 shows the absorption spectra of mycolactone A/B (red) and 2-naphthylboronate (blue) and the transparent region of the UV filter used (purple) [12].

These results therefore show that irradiation through a 365 nm filter can excite the pentanoate chromophore of mycolactone A/B but cannot excite 2-naphthylboronate.

In this assay, mycolactone A/B is detected as a yellow-green, fluorescent spot by excitation at 365 nm in cyclohexane-19, the pentanoate gives a fluorescence

emission at B 520 nm (green, yellow). Using our method, we observe the same patterns of the bacteria.

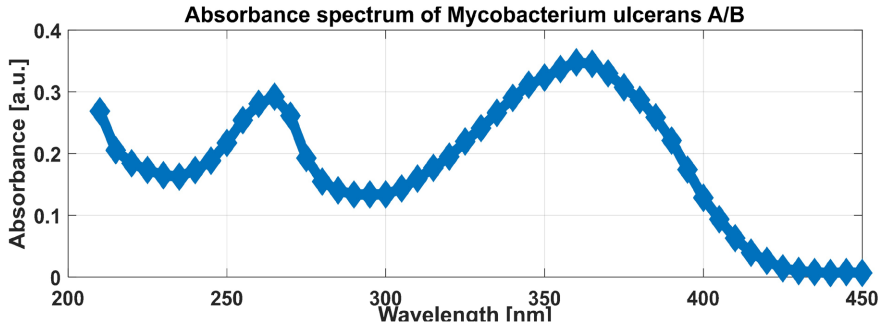

Figure 8. Absorbance spectrum of *Mycobacterium ulcerans* as a function of wavelength at 256 nm and 365 nm.

The device used reveals and detects the optical signature of the mycobacterium in Figure 8 which is the proof of the strong potential of our methodology in the early detection of this disease.

7. Analysis of the Results of the Sample Measurements

We then performed measurements on three selected skin sites with the LEDs sources. Site I: skin above the hand muscle, site II: skin above the wrist crease, and site III: skin on the back of the hand. The measurement for site I is shown in Figure 9.

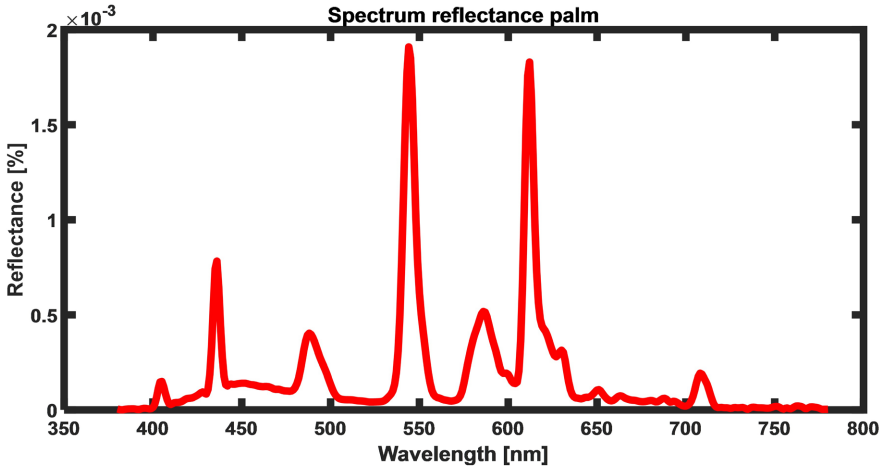

Figure 9. Evolution of the palm reflectance profile.

The analysis shows that the reflectance values are low with site I. The main reasons for this weakening could be the observed increasing low number of LED signal penetration for this measurement site located above the skin muscle. This led to a decrease in the sensitivity of the measurement site and a decrease in the specificities. Therefore, it is best to experiment with the characteristics of each site differently depending on the sensitivity of the site or its specific nature. Thus, we

evaluated sites II and III. The measurement results for site II are shown in Figure 10. For this site, we observed that the peaks are much larger at wavelengths where light is strongly absorbed by the chromophores. These spectral changes observed are consistent with the results of our study. Site I is less sensitive and less specific.

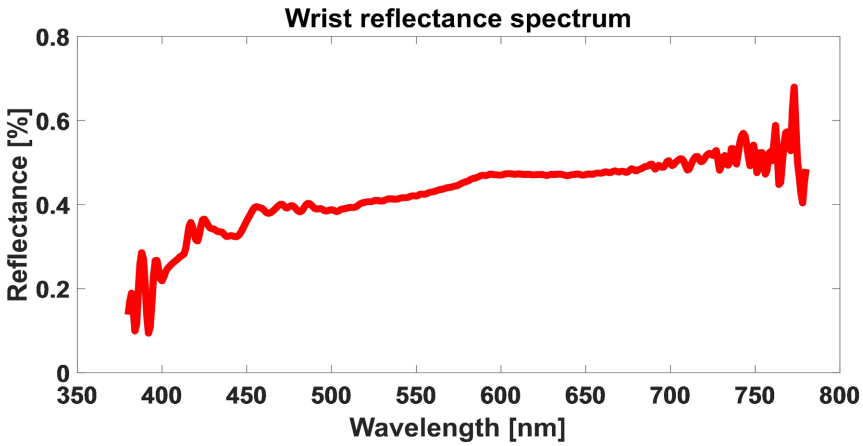

Figure 10. Evolution of the reflectance of the wrist of the hand.

Finally, Figure 11 shows the performance of our measurement evaluated over the entire range for site III. With respect to the optical window, we observed three significant peaks acquired at wavelengths 385 nm,420 nm and then the last peak at 773 nm respectively.

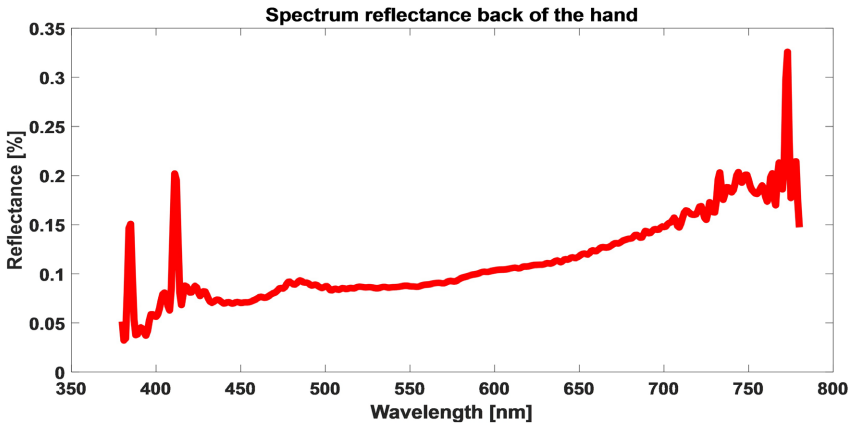

Figure 11. Spectral profile of the back of the hand.

These acquired peaks are induced by soft tissue can be used as a valuable source of additional information for diagnosis and characterization of biological tissues.

This data set will be useful for a variety of applications. For example, the data could be used for the development of physical and digital tissue phantoms or other models for human skin. Similarly, knowledge of the spectral reflectance signatures of human skin over a wide spectral range would assist in the development of imaging/detection systems used for emerging applications such as medical treatment and cosmetic technology.

Following our approach, further reflectance measurements were permed on various body parts of a person A and B in the spectral range 600 to 1200 nm and 1030 to 1300 nm. Analysis of the results obtained with the DRS instrument allows us to observe a growth in the diffuse reflectance spectra of various parts of the body of two persons A and B between the spectral ranges 600 and 750 nm and then 1030 and 1200 nm, respectively, Figure 12 and Figure 13. Whether it is person A or person B, we notice that the reflectance spectra of the areas with stain and scar are weak. Moreover, we note that the spectra have the same appearance, but they present different intensities.

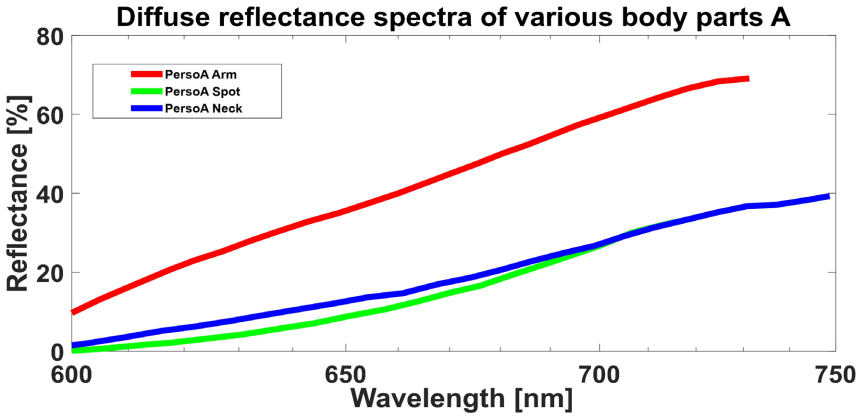

Figure 12. Diffuse reflectance spectra of various parts of the body of two separate individuals A and B.

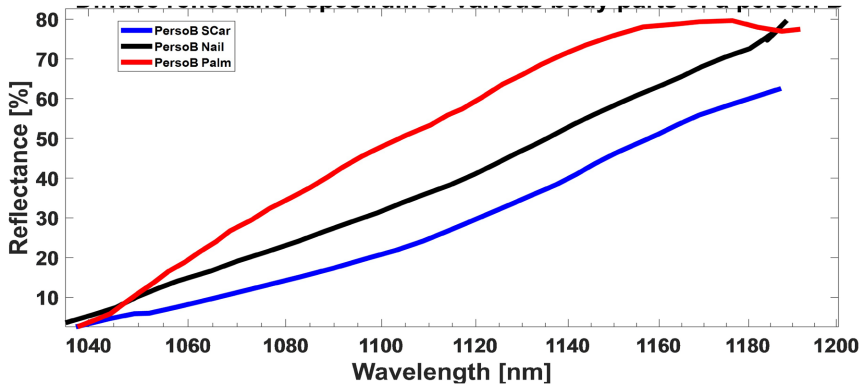

Figure 13. Diffuse spectra of various body parts of two persons A and B together.

On the other hand, there are hardly any peaks observed. Diffuse reflectance measurements from our device do show differences in spectra for various individuals. The differences are more distinct in terms of intensity. They also show spectral diagnosis is essential in the treatment of diseases, we think that it would be even more interesting to continue and finalize this project by a clinical experimentation so that results can be used for the diagnosis of other pathologies.

These satisfactory results show that the DRS is a method allowing to make diagnosis of this disease in situ. The approach presented here can finally be considered for use in diagnostic studies of this pathology based on the analysis of spectral

signatures and studies of skin chromophores. We acknowledge that our study has certain limitations, including the small size of the *in vivo* cohort, the use of tissue phantoms for certain acquisitions, and the limited diversity of skin types represented. Furthermore, the optical complexity of the skin as a scattering medium, the variability of *in vivo* and *ex vitro* measurements, and the limited penetration of certain wavelengths into the epidermis and dermis are also factors to consider. In order to overcome these constraints, we plan to conduct a larger-scale clinical validation, including a more diverse sampling of skin phototypes and an increased number of participants, in order to confirm and generalize the performance of our approach.

8. Conclusions

This study allowed us to propose and establish the basis for the development of a new non-invasive optical method to detect *Mycobacterium ulcerans* earlier, because the diagnosis of Buruli ulcer is still long, costly and traumatic for the patient (biopsy and transport).

Our approach is based on the diffuse reflectance spectroscopy that occurs when light passes through biological tissue. The first part of the study proposed an innovative instrumental solution to avoid the cost and pain of the invasive method. The proposed solution was developed through a prototype, and the performances were validated on an inert system and on people. The measurements carried out with this model allowed to quantify the reflectance. The coherent results obtained show the feasibility of this type of analytical method in early optical detection. The spectral information considered is consistent with the theoretical part of the absorption, reflection and scattering due to the interaction of the light wave with the biological tissue.

The developed system allows to obtain the spectral signature of this bacterium, according to the size of the particles and their biochemical composition, through the biological tissue without any trauma. This innovative approach provides information on the infected tissue, in depth and quantitatively, through the analysis of optical absorption and scattering properties. Diagnosis by this approach would consist in the analysis of spectral signatures.

In addition, this technique can be performed on site and implemented using compact and relatively inexpensive instruments, which is a significant advantage. This technique could be also considered for Buruli ulcer characterization in future biomedical applications.

Beyond the spectroscopy and physiological characterizations, the results obtained here can be placed in a more general perspective and the detailed analysis of skin health would allow a better understanding of the pathophysiology, the indolence associated with this disease.

Acknowledgements

The authors would like to thank Nordine Ouahabi, Arnauld Biganzoli, from the

electronic service of LAPLACE, Toulouse, France, for their help and realization of prototypes. We would like to express our gratitude to the CCA Service of the Ministry of State and Foreign Affairs of the French Embassy where their contribution and help are largely responsible for this success. We thank also the Pierre-Gennes Scientific Center for the training in frugal microscopy.

Conflicts of Interest

The authors declare no conflicts of interest regarding the publication of this paper.

References

[1] Roig, B. (2015) Caractérisation de tissus cutanés par spectroscopie bimodale: Réflectance Diffuse et Raman. PhD Thesis, Université de Reims Champagne Ardenne URCA. https://theses.hal.science/tel-01475307

[2] Jacques, S.L., Roman, J.R. and Lee, K. (2000) Imaging Superficial Tissues with Polarized Light. *Lasers in Surgery and Medicine*, **26**, 119-129. https://doi.org/10.1002/(sici)1096-9101(2000)26:2<119::aid-lsm3>3.0.co;2-y

[3] Steven Jacques. Google Scholar. https://scholar.google.com/citations?user=BkWNdX4AAAAJ&hl=fr&oi=sra

[4] Meglinski, I.V. and Matcher, S.J. (2002) Quantitative Assessment of Skin Layers Absorption and Skin Reflectance Spectra Simulation in the Visible and Near-Infrared Spectral Regions. *Physiological Measurement*, **23**, 741-753. https://doi.org/10.1088/0967-3334/23/4/312

[5] Prahl, S.A. (1999) Tabulated Molar Extinction Coefficient for Hemoglobin in Water. http://omlc.ogi.edu/spectra/hemoglobin/summary.html https://cir.nii.ac.jp/crid/1573105975606334464

[6] Duck, F.A. (1990) Physical Properties of Tissue. A Comprehensive Reference Book. https://cir.nii.ac.jp/crid/1572261549457803776

[7] Gandjbakhche, A.H. and Weiss, G.H. (1995) V: Random Walk and Diffusion-Like Models of Photon Migration in Turbid Media. In: *Progress in Optics*, Elsevier, 333-402. https://doi.org/10.1016/s0079-6638(08)70328-7

[8] Graaff, R., Dassel, A.C.M., Koelink, M.H., de Mul, F.F.M., Aarnoudse, J.G. and Zijlstra, W.G. (1993) Optical Properties of Human Dermis *in Vitro* and *in Vivo*. *Applied Optics*, **32**, 435-447. https://doi.org/10.1364/ao.32.000435

[9] Jacques, S.L. (2013) Corrigendum: Optical Properties of Biological Tissues: A Review. *Physics in Medicine and Biology*, **58**, 5007-5008. https://doi.org/10.1088/0031-9155/58/14/5007

[10] Garcia-Uribe, A., Smith, E.B., Zou, J., Duvic, M., Prieto, V. and Wang, L.V. (2011) *In-Vivo* Characterization of Optical Properties of Pigmented Skin Lesions Including Melanoma Using Oblique Incidence Diffuse Reflectance Spectrometry. *Journal of Biomedical Optics*, **16**, Article 020501.

[11] Spangenberg, T. and Kishi, Y. (2010) Highly Sensitive, Operationally Simple, Cost/Time Effective Detection of the Mycolactones from the Human Pathogen *Mycobacterium ulcerans*. *Chemical Communications*, **46**, 1410-1412. https://doi.org/10.1039/b924896j

[12] Converse, P.J., Xing, Y., Kim, K.H., Tyagi, S., Li, S.-Y., Almeida, D.V., *et al.* (2014) Accelerated Detection of Mycolactone Production and Response to Antibiotic Treatment in a Mouse Model of *Mycobacterium ulcerans* Disease. *PLOS Neglected Tropical Diseases*, **8**, e2618.

https://journals.plos.org/plosntds/article?id=10.1371/journal.pntd.0002618

[13] Sunar, U., Kress, J., Rohrbach, D. J., Carter, K. A., Luo, D., Shao, S., *et al.* (2016) Light-triggered Doxorubicin Release Quantified by Spatial Frequency Domain Imaging and Diffuse Optical Spectroscopy. In *Optical Tomography and Spectroscopy* (pp. JW4A-3). Optica Publishing Group. https://doi.org/10.1364/cancer.2016.jw4a.3

[14] Mazhar, A., Sharif, S.A., Cuccia, J.D., Nelson, J.S., Kelly, K.M. and Durkin, A.J. (2012) Spatial Frequency Domain Imaging of Port Wine Stain Biochemical Composition in Response to Laser Therapy: A Pilot Study. *Lasers in Surgery and Medicine*, **44**, 611-621. https://doi.org/10.1002/lsm.22067

[15] Fang, M.-H., Hsu, C.-S., Su, C., Liu, W., Wang, Y. and Liu, R. (2018) Integrated Surface Modification to Enhance the Luminescence Properties of K_2TiF_6:Mn^{4+} Phosphor and Its Application in White-Light-Emitting Diodes. *ACS Applied Materials & Interfaces*, **10**, 29233-29237. https://doi.org/10.1021/acsami.8b12170

[16] Schelkanova, I., Pandya, A., Shah, D., Lilge, L. and Douplik, A. (2014) Diffuse Reflectance Measurements Using Lensless CMOS Imaging Chip. *Journal of Physics*: *Conference Series*, **541**, Article ID: 012098. https://iopscience.iop.org/article/10.1088/1742-6596/541/1/012098/meta

[17] Foschum, F., Jäger, M. and Kienle, A. (2011) Fully Automated Spatially Resolved Reflectance Spectrometer for the Determination of the Absorption and Scattering in Turbid Media. *Review of Scientific Instruments*, **82**, Article ID: 103104. https://doi.org/10.1063/1.3648120

[18] Roig, B. (2015) Caractérisation de tissus cutanés par spectroscopie bimodale: Reflectance diffuse et Raman. Ph.D. Thesis, Université de Reims Champagne-Ardenne.